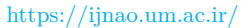
## Iranian Journal of Numerical Analysis and Optimization

Vol. 15, No. 4, 2025, pp 1589-1606

 $\rm https://doi.org/10.22067/ijnao.2025.95004.1712$ 







### Research Article



# A quadrature method for Volterra integral equations of the first kind



#### Abstract

This paper introduces a direct quadrature method for the numerical solution of Volterra integral equations of the first kind, utilizing a composite quadrature scheme based on the Floater–Hormann family of linear barycentric rational interpolants. The convergence of the proposed method is rigorously proved, and the order of convergence is explicitly derived in terms of the parameters of the method, thereby providing a clear theoretical framework for its performance. Several numerical experiments are provided to demonstrate both the efficiency and accuracy of the method, as well as to verify the excellent agreement between the implementation results and the theoretically predicted convergence rates.

AMS subject classifications (2020): Primary 65R20; Secondary 65D05.

**Keywords:** Volterra integral equations; Direct quadrature method; Rational interpolation; Barycentric form.

Received 19 August 2025; revised 4 September 2025; accepted 6 September 2025 Seyyed Ahmad Hosseini

Department of Mathematics, Faculty of Sciences, Golestan University, Gorgan, Iran. email: a.hosseini@gu.ac.ir

#### How to cite this article

## 1 Introduction

This paper is concerned with the numerical solution of the classical Volterra integral equations (VIEs) of the first kind

$$\int_{t_0}^t k(t, s, y(s)) \, \mathrm{d}s = g(t), \quad t \in I = [t_0, T], \tag{1}$$

where  $y: I \to \mathbb{R}$  is an unknown function, and  $k: S \times \mathbb{R} \to \mathbb{R}$  with  $S = \{(t,s): t_0 \leq s \leq t \leq T\}$ , represents the kernel of the equation. In practice, the functions g and k (except for its third variable) are typically used only at equispaced values of the variables. In what follows, we assume that  $g(t_0) = 0$ , and the functions g and k are smooth enough such that VIE (1) has a unique solution [21].

Volterra-type equations play a crucial role in modeling various dynamic systems where the current state of the system depends not only on its current conditions, but also on the accumulated effects of past interactions. In these equations, the related quantity varies in time and simultaneously depends on its past values. VIEs appear in various scientific and engineering disciplines, including physics, biology, engineering, and finance. For example, in viscoelasticity, they can describe how materials respond to stress over time, considering past deformations. In population dynamics, they help model species interactions by incorporating the influence of previous population levels. One of the notable applications of the first kind VIEs is in the field of epidemiology, particularly in the modeling of population dynamics during the spread of infectious diseases. Using VIEs in this context helps capture more realistically the interaction between susceptible, infected, and recovered individuals over time, incorporating the history of infection events and their cumulative effect on the population.

Most real-world problems are so complicated that there is no hope of finding an analytical solution. As a result, numerical methods are often needed to obtain solutions. Specifically, Volterra-type equations also necessitate numerical methods that yield approximations to the exact solutions. The development of a numerical solver for VIEs is a wide and mature area of research; see for instance [9, 10, 21] and the references therein.

A broad range of numerical methods across various classes has been developed for VIEs of the first kind (see, e.g., [13, 15, 26]). For smooth kernels, first-kind VIEs can be transformed into equivalent second-kind equations. Where the kernels are explicitly defined and differentiable, suitable numerical techniques tailored for second-kind VIEs can be applied, ensuring more efficient and accurate solutions.

Direct quadrature methods are among the simplest and most traditional schemes for solving VIEs. These methods commonly employ composite Newton–Cotes formulas, Gregory's rules, and hybrid schemes, providing a clear and efficient strategy for the numerical solution of VIEs. Nevertheless, their effectiveness diminishes when higher accuracy is required. They also often exhibit instability and loss of precision, particularly when applied to problems with smooth kernels over long intervals or under conditions of increasing mesh density. Moreover, it is important to note that, as the degree of the method increases, these schemes can suffer from Runge's phenomenon, wherein oscillations lead to significant numerical errors, and making them impractical [12].

A more robust alternative is to replace polynomial interpolation, which forms the foundation of many traditional numerical methods, with linear barycentric rational interpolation, which is characterized by barycentric weights, one for every node. The weights are chosen in such a way that bad properties of the polynomial such as ill-conditioning and Runge's phenomenon are avoided, and convergence, well-conditioning and absence of poles are guaranteed. Berrut [5] presented a very simple choice of the barycentric weights that successfully avoids poles in the interpolation interval. However, despite the excellent conditioning of the resulting linear barycentric rational interpolants (LBRIs), their convergence rate remains slow for general node distributions. The situation changed significantly with the introduction of a new family of LBRIs by Floater and Hormann in [11], a family of barycentric rational interpolants based on a blend of the local polynomial interpolants, which depends on a parameter d, and including the previously introduced interpolants. This family of LBRIs presents a favorable comparison to more classical polynomial interpolants, for interpolation of univariate data, especially in the equispaced setting. Indeed,

the Lebesgue constant associated with these interpolants exhibits logarithmic growth in this situation, a stark contrast to the exponential growth experienced by polynomials. This logarithmic growth implies that the error increases at a much slower rate, and making them more advantageous for accurate interpolation in such settings compared to classical polynomial interpolants [7, 8]. Moreover, the flexibility, robustness, and favorable convergence rate, make these tools a state-of-the-art method for interpolation at equispaced nodes. Due to these attractive features, this family of LBRIs has recently gained popularity and has been used in the construction of various numerical methods for solving different classes of time-dependent problems [1, 2, 3, 4, 6, 18, 19, 20, 22, 23]. The spirit of this paper is that of deriving a highly accurate and stable scheme based on the composite barycentric rational quadrature (CBRQ) introduced in [6] for the numerical solution of VIEs of the first kind (1).

After briefly reviewing the LBRIs in Section 2, a method for solving VIEs (1) based on the CBRQ rule will be introduced in Section 3. This section further provides a rigorous convergence analysis of the method and its order of accuracy. The robustness and efficiency of the method and the theoretical results on its order of convergence are illustrated by some numerical experiments in Section 4.

# 2 Linear barycentric rational quadrature

Quadrature formulas constitute a fundamental component of simulation, data analysis, and numerical modeling, playing a vital role in addressing practical problems across many fields of computational sciences and engineering. A natural and widely adopted approach for approximating the definite integral of a function over a bounded interval is to replace the integrand with a suitable interpolant and apply the integration operator to the resulting approximation. In particular, linear interpolation schemes trivially lead to quadrature rules through this process. Prior to reviewing the idea underlying the CBRQ rule, we first give a short introduction to the Floater–Hormann family of LBRIs.

Let f be a real-valued and continuously differentiable function over the interval [a, b], and consider the n + 1 distinct interpolation nodes

$$a = t_0 < t_1 < \dots < t_n = b.$$

The Floater–Hormann family of the LBRIs to interpolate the given n+1 pairs  $(t_j, f(t_j))$ , with distinct nodes  $t_j, j = 0, 1, \ldots, n$ , for every fixed nonnegative integer  $d \leq n$ , takes the barycentric form [11]

$$r_{n,d}[f](t) = \sum_{k=0}^{n} b_k^{(n,d)}(t)f(t_k), \quad b_k^{(n,d)}(t) = \frac{\beta_k^{(n,d)}}{t - t_k} / \sum_{j=0}^{n} \frac{\beta_j^{(n,d)}}{t - t_j}, \quad (2)$$

with the barycentric weights

$$\beta_k^{(n,d)} = \sum_{i=\max(0,k-d)}^{\min(k,n-d)} (-1)^i \prod_{j=i, j \neq k}^{i+d} \frac{1}{t_k - t_j},\tag{3}$$

where  $0 \le d \le n$ . We denote the function to be interpolated by f, to avoid confusion with the functions g and g in VIE (1). The following theorem from [11] gives the rate of convergence of this family of the LBRIs via a bound on the interpolation error in the maximum norm.

**Theorem 1.** For any  $f \in C^{d+2}[a,b]$ , we have

$$||r_{n,d}[f] - f|| \le Ch^{d+1},$$

where  $h = \max_{0 \le k \le n-1} (t_{k+1} - t_k)$  is the global mesh size and the constant C depends only on d, the derivatives of f, the interval length b-a, and, only in the case d = 0, on the maximal local mesh ratio

$$\rho = \max_{1 \le k \le n-2} \min \left\{ \frac{t_{k+1} - t_k}{t_k - t_{k-1}}, \frac{t_{k+1} - t_k}{t_{k+2} - t_{k+1}} \right\}.$$

Moreover, according to [11, Theorem 2], in the case of odd n-d, the bound on the interpolation error involves an additional factor, nh, so the order of convergence is one unit larger than the stated above, that is,  $d+1+\delta$ , where  $\delta=1$  for odd n-d and  $\delta=0$  for even n-d.

Throughout this work, we are mainly interested in the case of uniformly spaced nodes, when the weights in (3) can be replaced by

$$\bar{\beta}_k^{(n,d)} = (-1)^d d! \, h^d \beta_k^{(n,d)} = (-1)^k \sum_{i=d}^n \binom{d}{i-k}, \qquad k = 0, 1, \dots, n.$$
 (4)

The linearity of barycentric rational interpolation in data renders it well-suited for applications. Klein and Berrut [17] introduced a global quadrature formula based on integrating the LBRI (2) corresponding to the real integrable function f over the integration interval [a, b] of the form

$$\int_{a}^{b} f(t) dt \approx \int_{a}^{b} r_{n,d}[f](t) dt$$

$$= h \sum_{k=0}^{n} w_{n,k} f_{k} = Q_{n}^{G},$$
(5)

with quadrature weights

$$w_{n,k} = h^{-1} \int_{a}^{b} b_{k}^{(n,d)}(t) dt = \int_{0}^{n} \phi_{k}^{(n,d)}(x) dx,$$
 (6)

where

$$\phi_k^{(n,d)}(x) = \frac{\bar{\beta}_k^{(n,d)}}{x-k} / \sum_{j=0}^n \frac{\bar{\beta}_j^{(n,d)}}{x-j},$$

with  $\bar{\beta}_k^{(n,d)}$  as in (4).

The integrands in (6) are rational functions that, in general, cannot be integrated analytically without additional knowledge of their properties, such as the locations of their poles. Furthermore, algebraic methods typically require the polynomials in the numerator and denominator of the integrand to be in canonical form, a representation often impaired by stability issues. As a result, these integrals must be computed numerically up to machine precision, using, for instance, the routines available in the Chebfun system [24] or, alternatively, with Gauss–Legendre or Clenshaw–Curtis quadrature rules [14, 25]. Notably, the barycentric form exhibits greater flexibility compared to Gauss–Legendre quadrature, as it allows for arbitrary node distributions rather than restricting nodes to the roots of Legendre polynomials. Moreover,

barycentric rational quadrature is particularly effective at handling endpoint singularities and functions with steep gradients, owing to its basis in rational approximation.

The convergence and stability of the resulting quadrature rule directly inherit the corresponding properties of the underlying interpolant. It was proved in [17] that for nonnegative integers n and d,  $d \le n/2 - 1$ , and  $f \in C^{d+3}[a,b]$ , the quadrature formula (5) with quadrature weights (6) converges at the rate  $O(h^{d+2})$  as the global mesh size h tends to zero if the quadrature weights given by (6) are approximated by a quadrature rule converging at least at the rate  $O(h^{d+2})$ .

Direct application of the quadrature formula in discretization schemes for time-dependent problems, specifically VIEs, implies significant computational cost due to the necessity of computing quadrature weights at each time step as the partition size grows. However, since the barycentric weights (6) do not depend on the nodes and are translation invariant, it is possible to develop a composite version of the quadrature rule that addresses this issue efficiently.

Consider the interval [a,b] partitioned uniformly by points  $a=t_0 < t_1 < \cdots < t_N = b$  with step size  $h = \frac{b-a}{N}$ , so that  $t_k = a + kh$  for  $k = 0, 1, \ldots, N$ . Let d and n satisfy  $0 \le d \le n \le N/2$ , and define  $p = \lfloor \frac{N}{n} \rfloor - 1$ . Under these conditions, the CBRQ rule can be formulated as

$$\int_{t_0}^{t_N} f(t) dt = \sum_{j=0}^{p-1} \int_{t_{jn}}^{t_{(j+1)n}} f(t) dt + \int_{t_{pn}}^{t_N} f(t) dt$$

$$\approx h \sum_{j=0}^{p-1} \sum_{k=0}^{n} w_{n,k} f_{jn+k} + h \sum_{k=0}^{N-pn} w_{N-pn,k} f_{pn+k} = Q_N^C, \qquad (7)$$

where

$$w_{i,k} = h^{-1} \int_{t_0}^{t_i} b_k^{(i,d)}(t) dt = \int_0^i \phi_k^{(i,d)}(x) dx,$$
 (8)

for i = n, n + 1, ..., 2n - 1 and k = 0, ..., i. Note that for  $n \le N \le 2n$ , the only contributing term in (7) is the last one, which is precisely the global quadrature formula given in (5).

Based on this construction, and noting that each local quadrature formula converges at the rate of  $O(h^{d+2})$ , and that n is fixed and there are p+1=

O(n) = O(1/h) integrals to be computed, the order of the CBRQ rule (7) behaves as follows.

**Theorem 2.** Suppose that N and n are positive integers with  $n \leq N$ , that d is a nonnegative integer with  $d \leq n \leq N/2$ , and that  $f \in C^{d+2}[a,b]$ . Then the absolute error in the approximation of the integral of f with the composite quadrature rule (7) goes to zero as  $O(h^{d+1+\delta})$ , where  $\delta = 0$  if n-d is even and  $\delta = 1$  if n-d is odd.

# 3 Description of the method for VIEs of the first kind

In this section, we utilize the favorable properties of the introduced CBRQ rule, including smoothness, high accuracy, and an arbitrarily high rate of convergence, to construct a direct quadrature-based scheme for numerically solving the classical VIEs of the form (1). Differentiating (1) yields VIEs of the second kind

$$k(t, t, y(t)) + \int_{t_0}^{t} k_t(t, s, y(s)) ds = g'(t), \quad t \in I,$$
 (9)

where  $k_t$  is the partial derivative of the kernel k with respect to t.

Let  $T_N = \{t_0, t_1, \dots, t_N = T\}$  be a uniform partition of the given interval I with the fixed stepsize  $h = t_{i+1} - t_i = (T - t_0)/N$ ,  $i = 0, 1, \dots, N - 1$  and assume that d and n are as introduced in section 2, and that  $p = \lfloor m/n \rfloor - 1$ . Applying the CBRQ rule (7) to the integral part of (9) at the mesh point  $t_m$  yields

$$k(t_m, t_m, y_m) + h \sum_{j=0}^{p-1} \sum_{k=0}^{n} w_{n,k} k_t(t_m, t_{jn+k}, y_{jn+k})$$

$$+ h \sum_{k=0}^{m-pn} w_{m-pn,k} k_t(t_m, t_{pn+k}, y_{pn+k}) = g'(t_m),$$
(10)

for m = n + 1, ..., N. The quadrature weights  $w_{i,k}$  are given by (8) for i = n, n + 1, ..., 2n - 1 and k = 0, ..., i. Here  $y_m$  denotes the approximation to the exact solution y of (1) at  $t = t_m$ . This approach will be referred to as

the CBRQM, which stands for "composite barycentric rational quadrature method".

It is clear that a set of starting values  $y_m$ , m = 1, 2, ..., n, is necessary to prevent deterioration in the order of convergence of the method, as any loss of precision will be carried over through the whole interval of integration. To supply them, we employ the quadrature formula (5) to approximate the integral part of (9) over the interval  $[t_0, t_m]$ , m = 1, 2, ..., n, which gives

$$k(t_m, t_m, y_m) + h \sum_{k=0}^{n} \overline{w}_{m,k} k_t(t_m, t_k, y_k) = g'(t_m),$$
 (11)

where the quadrature weights required for the starting procedure are given by

$$\overline{w}_{m,k} = \int_0^m \frac{\bar{\beta}_k^{(n,d)}}{x-k} / \sum_{j=0}^n \frac{\bar{\beta}_j^{(n,d)}}{x-j} dx, \quad k = 0, 1, \dots, n,$$

wherein the barycentric weights  $\bar{\beta}_j^{(n,d)}$  depend on n, not on m. This starting procedure is fully implicit and specifically designed to provide sufficiently accurate starting values. It is essential to emphasize that the nonlinear system of equations represented by (11) contains n equations in the n unknowns  $y_m$ ,  $m = 1, 2, \ldots, n$ . This system must be solved simultaneously to obtain the starting values required for the subsequent implementation of the method. The following theorem rigorously establishes the convergence rate of the starting values derived from (11) in terms of the parameters of the method.

**Theorem 3.** Assume that  $f \in C^{d+2}(I)$  and  $k \in C^{d+2}(S \times \mathbb{R})$ , let  $\mathbf{y}_n = (y_1, y_2, \dots, y_n)^T$  be the approximate values obtained by the starting procedure (11) with  $d \leq n$ , and let  $\mathbf{e}_n = (e_1, e_2, \dots, e_n)^T$ , where  $e_i = y(t_i) - y_i$ ,  $i = 1, 2, \dots, n$ , are the starting errors. Then,  $\|\mathbf{e}_n\|_{\infty}$  goes to zero as  $O(h^{d+2+\delta})$ , where  $\delta = 0$  for even values of n - d and  $\delta = 1$  for odd values of n - d.

*Proof.* Substituting the exact values for y in the starting procedure (11) and incorporating their consistency error  $R_m(h)$  gives

$$k(t_m, t_m, y(t_m)) + h \sum_{k=0}^{n} \overline{w}_{m,k} k_t(t_m, t_k, y(t_k)) + R_m(h) = g'(t_m).$$
 (12)

Subtracting equation (9), in which the variable t is replaced by  $t_m$ , from (12) for each m = 1, 2, ..., n, yields

$$R_m(h) = \int_{t_0}^{t_m} k_t(t_m, s, y(s)) \, \mathrm{d}s - h \sum_{k=0}^n \overline{w}_{m,k} \, k_t(t_m, t_k, y(t_k)).$$

Since  $m \leq n$ , n is constant, and h shrinks, it readily follows from the convergence rate of the global quadrature (5) that for each m = 1, 2, ..., n,  $R_m(h) = O(h^{d+2})$ . Considering the arguments mentioned just after Theorem 1, it can be deduced that when n-d is odd, the convergence order of the starting values increases by one, yielding  $d+2+\delta$ , where  $\delta$  is the same quantity as stated in Theorem 2.

Subtracting the starting values in (11) from (12) and using the mean value theorem gives

$$k_y(t_m, t_m, \xi_m)e_m + h \sum_{k=0}^n \overline{w}_{m,k} k_{ty}(t_m, t_k, \eta_k)e_k = R_m(h), \quad m = 1, 2, \dots, n,$$

where  $k_y$  and  $k_{ty}$  denote the partial derivatives of k with respect to y and t, y, respectively, and where  $\xi_m$  and  $\eta_k$  lie within the interior of the line segments connecting the exact value of y and its approximations at the corresponding functions. Introducing the matrix  $\mathcal{D}_n$  as the diagonal matrix with entries  $k_y(t_m, t_m, \xi_m)$  for m = 1, 2, ..., n, the matrix  $\mathcal{W}_n$  with the (m, k)th element given by  $\overline{w}_{m,k} k_{ty}(t_m, t_k, \eta_k)$ , and the consistency error vector  $\mathbf{R}_n(h) := [R_1(h), R_2(h), ..., R_n(h)]^T$ , the last equation can be written in matrix form as

$$(\mathcal{D}_n + h\mathcal{W}_n)\mathbf{e}_n = \mathbf{R}_n(h).$$

Due to the differentiability assumption on the kernel k, the partial derivatives involved in the matrices have a maximum absolute value, and since n is fixed in the starting procedure (11) and only the stepsize h varies, the corresponding starting quadrature weights remain bounded as well. Consequently, the norm of the matrix  $W_n$  is bounded so that  $h \|W_n\|_{\infty}$  may be made as small

as necessary by diminishing h. Therefore, with small enough stepsize h, there exists a positive constant C such that

$$\|\mathbf{e}_{n}\|_{\infty} \leq \|(\mathcal{D}_{n} + h\mathcal{W}_{n})^{-1}\|_{\infty} \|\mathbf{R}_{n}(h)\|_{\infty}$$

$$\leq \frac{1}{\|\mathcal{D}_{n}\|_{\infty} - h \|\mathcal{W}_{n}\|_{\infty}} \|\mathbf{R}_{n}(h)\|_{\infty}$$

$$\leq C \|\mathbf{R}_{n}(h)\|_{\infty},$$

which implies  $\|\mathbf{e}_n\|_{\infty} = O(h^{d+2+\delta})$ .

We are now in a position to state our main theorem about the order of convergence of the method (10), which can easily be deduced with the same ingredients as in [21, Theorem 7.2], and the help of Theorems 2 and 3.

**Theorem 4.** Let  $g \in C^{d+2}(I)$  and let  $k \in C^{d+2}(S \times \mathbb{R})$ , where the kernel k satisfies a Lipschitz condition with respect to its third argument. Assume further that n and d with  $d \leq n$  are,respectively positive and nonnegative integers, and let the nodes be equispaced. Then, the CBRQM (10) is convergent of order  $d+1+\delta$  if the order of the utilized starting procedure is at least  $d+\delta$ , where  $\delta=0$  for even values of n-d, and  $\delta=1$  for odd values of n-d.

# 4 Numerical experiments

In this section, we apply the proposed method with various choices of n, d, and  $d_s$  (for the starting procedure), to several linear and nonlinear VIEs of the first kind to illustrate the efficiency and accuracy of the method and verify the theoretical convergence estimates established in section 3. To this end, the approximation quality in each numerical experiment is measured by

$$e_h^S = \max_{1 \le m \le n} ||y(t_m) - y_m||_{\infty},$$

the maximum norm of the starting errors, and

$$e_h(T) = ||y(t_N) - y_N||_{\infty},$$

the maximum norm of the error at the endpoint  $t_N = T$  of the integration interval. Additionally, to validate the theoretical convergence order, the experimental estimate of the order of accuracy for the starting procedure (11) and the CBRQM (10) are computed by

$$O_S = \log_2(e_h^S/e_{h/2}^S),$$

and

$$O_C = \log_2(e_h^C(T)/e_{h/2}^C(T)).$$

As a first example, consider the linear convolution VIE of the first kind [13]

$$\int_0^t (c^2 + 1)\cos(t - s)y(s) \, ds = ce^{ct} + \sin t - c\cos t, \quad t \in [0, 4],$$
 (13)

where  $c=\pm 1$ , and the exact solution is given by  $y(t)=e^t$ . Tables 1 and 2 list numerical results for the starting procedure and the CBRQM with various choices of the parameters  $(n,d,d_s)$  and different values of the stepsize h. For both cases of the parameter c, the errors decrease with decreasing stepsize h. As to be expected from Theorem 3, the error of the starting values decreases at the rate of  $d_s + 2 + \delta$ , with  $\delta = 1$  for odd  $n - d_s$  and  $\delta = 0$  for even  $n - d_s$ , and the errors of the CBRQM (10) decrease at the rate of  $d + 1 + \delta$ , with  $\delta = 1$  for odd n - d and  $\delta = 0$  for even n - d, as established by Theorem 4.

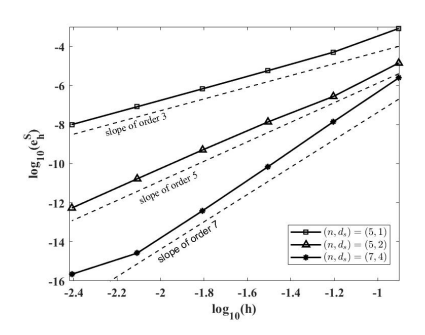
Table 1: Numerical results of the CBRQM applied to the VIE in (13) with c=1.

h		2-2	$2^{-3}$	$2^{-4}$	$2^{-5}$	$2^{-6}$	$2^{-7}$	$2^{-8}$
$(n, d, d_s) = (5, 2, 1)$								
Starting procedure	$e_h^S$	5.90e-3	$4.63e{-4}$	$4.76\mathrm{e}{-5}$	$5.46\mathrm{e}{-6}$	$6.54\mathrm{e}{-7}$	$8.02e{-8}$	9.92e - 9
	$O_S$		3.67	3.28	3.12	3.06	3.03	3.02
CBRQM	$e_h^C(T)$	1.72e-2	$1.26e{-3}$	$7.73e{-5}$	$4.69e{-6}$	$2.94e{-7}$	$1.84e{-8}$	$1.15e{-9}$
	$O_C$		3.77	4.03	4.04	4.00	4.00	4.00
$(n, d, d_s) = (6, 3, 2)$								
Starting procedure	$e_h^S$	8.28e-4	$3.18\mathrm{e}{-5}$	$1.48e{-6}$	$7.96e{-8}$	$4.60e{-9}$	$2.77e{-10}$	$1.70e{-11}$
	$O_S$		4.70	4.43	4.22	4.11	4.05	4.03
CBRQM	$e_h^C(T)$	1.02e-3	$2.39e{-5}$	$7.55e{-7}$	$2.78e{-8}$	1.03e - 9	$3.52e{-11}$	$1.15\mathrm{e}{-12}$
	$O_C$		5.42	4.98	4.76	4.75	4.87	4.94

As the second test problem, consider the classical VIE of the form [16]

h		2-2	$2^{-3}$	$2^{-4}$	$2^{-5}$	$2^{-6}$	$2^{-7}$	$2^{-8}$
$(n,d,d_s) = (5,2,1)$								
Starting procedure	$e_h^S$	$1.50e{-3}$	$2.43\mathrm{e}{-4}$	$3.48\mathrm{e}{-5}$	$4.66e{-6}$	$6.05\mathrm{e}{-7}$	$7.71e{-8}$	9.73e - 9
	$O_S$		2.63	2.80	2.90	2.95	2.97	2.99
CBRQM	$e_h^C(T)$	3.10e-3	$2.91e{-4}$	$2.18e{-5}$	$1.49e{-6}$	$9.74e{-8}$	$6.22e{-9}$	$3.93e{-10}$
	$O_C$		3.41	3.74	3.87	3.94	3.97	3.98
$(n, d, d_s) = (6, 3, 2)$								
Starting procedure	$e_h^S$	1.75e-4	$1.43\mathrm{e}{-5}$	$1.00e{-6}$	$6.57\mathrm{e}{-8}$	$4.19e{-9}$	$2.64 \mathrm{e}{-10}$	$1.66e{-11}$
	$O_S$		3.61	3.84	3.93	3.97	3.99	3.99
CBRQM	$e_h^C(T)$	2.21e-4	$1.91e{-5}$	$9.06e{-7}$	$3.39e{-8}$	1.15e - 9	$3.75e{-11}$	$1.19e{-12}$
	$O_C$		3.53	4.40	4.74	4.88	4.94	4.98

Table 2: Numerical results of the CBRQM applied to the VIE in (13) with c = -1.



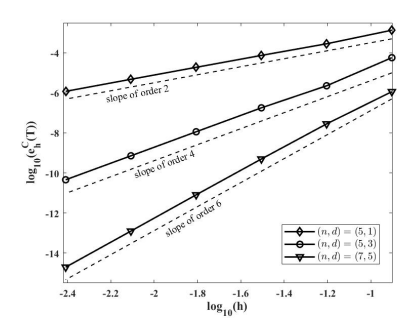


Figure 1: Log-log-plots of the approximation error of the starting procedure and the CBRQM applied to the VIE in (14) with  $(n, d_s) = (5, 1), (5, 2), (7, 4)$  (left) and (n, d) = (5, 1), (5, 3), (7, 5) (right).

$$\int_{0}^{t} e^{-ts} y(s) \, \mathrm{d}s = g(t), \quad t \in [0, 1], \tag{14}$$

where the function g is chosen such that the exact solution is  $y(t) = e^{-t} \cos t$ . Figure 1 shows the logarithmic errors  $\log_{10}(e_h^S)$  and  $\log_{10}(e_h^C(T))$  of the starting procedure and the CBRQM (10) for this equation, plotted versus  $\log_{10}(h)$ , together with the slope lines corresponding to the expected convergence rates. The numerical results confirm the expected orders of convergence for various choices of  $(n,d,d_s)$  as predicted by Theorems 3 and 4.

To demonstrate the efficiency and accuracy of the CBRQM (10), consider the following nonlinear first-kind VIE

$$\int_0^t \frac{1}{t+s+9+e^{y(s)}} \, \mathrm{d}s = \frac{1}{2} \log \left( \frac{3t+10}{t+10} \right), \quad t \in [0,1], \tag{15}$$

Iran. J. Numer. Anal. Optim., Vol. 15, No. 4, 2025, pp 1589-1606

with the exact solution  $y(t) = \log(t+1)$ . The numerical results for this equation are presented in Table 3 for the parameter  $(n, d, d_s) = (3, 1, 1)$  and  $(n, d, d_s) = (8, 3, 2)$ . These results clearly validate the theoretical convergence order of the proposed method.

h		2-3	$2^{-4}$	$2^{-5}$	$2^{-6}$	$2^{-7}$	$2^{-8}$
$(n,d,d_s) = (3,1,1)$							
Starting procedure	$e_h^S$	2.71e-5	$3.97\mathrm{e}{-6}$	$5.44\mathrm{e}{-7}$	$7.13e{-8}$	$9.14e{-9}$	$1.16\mathrm{e}{-9}$
	$O_S$		2.77	2.87	2.93	2.96	2.98
CBRQM	$e_h^C(T)$	$3.66e{-5}$	$9.51e{-6}$	$2.79e{-6}$	$7.02\mathrm{e}{-7}$	$1.82\mathrm{e}{-7}$	$4.55\mathrm{e}{-8}$
	$O_C$		1.94	1.77	1.99	1.95	2.00
$(n,d,d_s) = (8,3,2)$							
Starting procedure	$e_h^S$	1.12e-6	$8.42\mathrm{e}{-8}$	$5.83\mathrm{e}{-9}$	$3.85\mathrm{e}{-10}$	$2.48e{-11}$	$1.57\mathrm{e}{-12}$
	$O_S$		3.73	3.85	3.92	3.96	3.98
CBRQM	$e_h^C(T)$	1.88e-7	$4.57\mathrm{e}{-9}$	$1.68e{-10}$	$5.74e{-12}$	$1.87e{-13}$	$5.33e{-15}$
	$O_C$		5.36	4.77	4.87	4.94	5.13

Table 3: Numerical results of the CBRQM applied to the VIE in (15).

Implementation of numerical methods becomes increasingly challenging when dealing with VIEs over long integration intervals. To demonstrate the efficiency of the CBRQM in such cases, consider the nonlinear VIE

$$\int_0^t \sin(t - sy(s)) \, \mathrm{d}s = 1 - \cos t, \quad t \in [0, 100], \tag{16}$$

where the exact solution is y(t) = 1. The numerical results for this equation with parameters  $(n, d, d_s) = (10, 3, 2)$  and  $(n, d, d_s) = (12, 5, 4)$  are given in Table 4 and confirm once more the theoretical results and the capability of the method in solving VIEs over long intervals.

Finally, consider the highly oscillatory first-kind VIE

$$\int_{0}^{t} e^{-\alpha(t-s)} \cos(\omega(t-s)) y(s) \, \mathrm{d}s = g(t), \quad t \in [0,1], \tag{17}$$

where the function g is chosen such that the exact solution is  $y(t) = e^{-\alpha t} \sin(\omega t)$ . For  $\alpha > 0$  and  $\omega \gg 1$ , the VIE in (17) becomes highly oscillatory due to the cosine term. Figure 2 shows the logarithmic errors  $\log_{10}(e_h^S)$  and  $\log_{10}(e_h^C(T))$ , corresponding to the starting procedure and the CBRQM (10), applied to the VIE in (17) for  $\alpha = 1$  and  $\omega = 100$ , plotted versus

h		2-2	$2^{-3}$	$2^{-4}$	$2^{-5}$	$2^{-6}$	$2^{-7}$
$(n,d,d_s) = (10,3,2)$							
Starting procedure	$e_h^S$	$2.20e{-4}$	$2.18\mathrm{e}{-5}$	$1.51\mathrm{e}{-6}$	$9.67e{-8}$	6.08e - 9	$3.80\mathrm{e}{-10}$
	$O_S$		3.34	3.85	3.96	3.99	4.00
CBRQM	$e_h^C(T)$	$7.36e{-5}$	$1.48e{-5}$	$9.03e{-7}$	$3.32e{-8}$	$1.08e{-9}$	$3.41e{-11}$
CBRQM	$O_C$		2.31	4.03	4.77	4.94	4.99
$(n, d, d_s) = (12, 5, 4)$							
Starting procedure	$e_h^S$	$8.01e{-6}$	$2.26\mathrm{e}{-7}$	$4.01e{-9}$	$6.46 \mathrm{e}{-11}$	$1.02e{-12}$	$1.55\mathrm{e}{-14}$
	$O_S$		5.15	5.82	5.96	5.98	6.04
CBRQM	$e_h^C(T)$	4.89e - 6	$1.01e{-7}$	2.34e - 9	$2.44e{-11}$	$2.12e{-13}$	$1.55 \mathrm{e}{-15}$
	$O_C$		5.60	5.43	6.58	6.85	7.10

Table 4: Numerical results of the CBRQM applied to the VIE in (16).

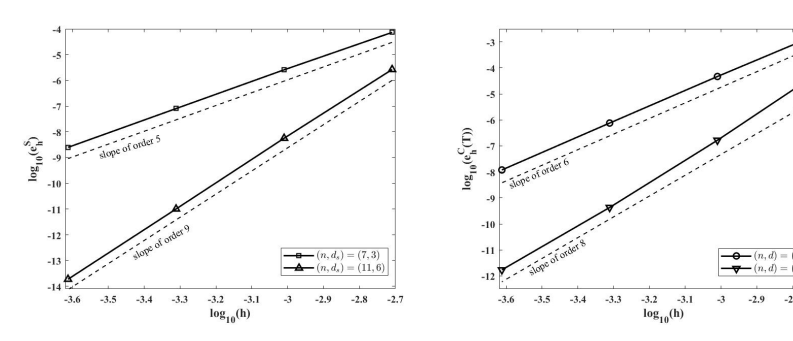


Figure 2: Log-log-plots of the approximation error of the starting procedure and the CBRQM applied to the VIE in (17) with  $(n, d_s) = (7, 3), (11, 6)$  (left) and (n, d) = (7, 4), (11, 7) (right).

 $\log_{10}(h)$ , together with the expected convergence rates. As expected, the experimental orders of convergence for both the starting procedure and the CBRQM (10) exhibit excellent agreement with the theoretical results.

# References

- Abdi, A., Arnold, M. and Podhaisky, H. The barycentric rational numerical differentiation formulas for stiff ODEs and DAEs, Numer. Algorithms 97 (2024), 431–451.
- [2] Abdi, A., Berrut, J.-P. and Podhaisky, H. The barycentric rational predictor-corrector schemes for Volterra integral equations, J. Comput.

- Appl. Math. 440 (2024), 115611.
- [3] Abdi, A. and Hosseini, S.A. The barycentric rational differencequadrature scheme for systems of Volterra integro-differential equations, SIAM J. Sci. Comput. 40 (2018), A1936–A1960.
- [4] Abdi, A., Hosseini, S.A. and Podhaisky, H. The linear barycentric rational backward differentiation formulae for stiff ODEs on nonuniform grids, Numer. Algorithms 98 (2025), 877–902.
- [5] Berrut, J.-P. Rational functions for guaranteed and experimentally well-conditioned global interpolation, Comput. Math. Appl. 15 (1998), 1–16.
- [6] Berrut, J.-P., Hosseini, S.A. and Klein, G. The linear barycentric rational quadrature method for Volterra integral equations, SIAM J. Sci. Comput. 36 (2014), A105–A123.
- [7] Bos, L., De Marchi, S. and Hormann, K. On the Lebesgue constant of Berrut's rational interpolant at equidistant nodes, J. Comput. Appl. Math. 236 (2011), 504–510.
- [8] Bos, L., De Marchi, S., Hormann, K. and Klein, G. On the Lebesgue constant of barycentric rational interpolation at equidistant nodes, Numer. Math. 121 (2012), 461–471.
- [9] Brunner, H. Collocation Methods for Volterra Integral and Related Functional Equations, Cambridge University Press, Cambridge, 2004.
- [10] Brunner, H. and van der Houwen, P.J. The Numerical Solution of Volterra Equations, in: CWI Monogr., North-Holland, Amsterdam, 1986.
- [11] Floater, M.S. and Hormann, K. Barycentric rational interpolation with no poles and high rates of approximation, Numer. Math. 107 (2007), 315–331.
- [12] Fornberg, B. and Reeger, J.A. An improved Gregory-like method for 1-D quadrature, Numer. Math. 141 (2019), 1–19.

- [13] Gladwin, C.J. Quadrature rule methods for Volterra integral equations of the first kind, Math. Comput. 33 (1979), 705–716.
- [14] Hale, N. and Townsend, A. Fast and accurate computation of Gauss– Legendre and Gauss–Jacobi quadrature nodes and weights, SIAM J. Sci. Comput. 35 (2013), A652–A674.
- [15] Holyhead, P.A.W., McKee, S. and Taylor, P.J. Multistep methods for solving linear Volterra integral equations of the first kind, SIAM J. Numer. Anal. 12 (1975), 698–711.
- [16] Kauthen, J.-P. and Brunner, H. Continuous collocation approximations to solution of first kind Volterra equations, Math. Comput. 66 (1997), 1441–1459.
- [17] Klein, G. and Berrut, J.-P. Linear barycentric rational quadrature, BIT 52 (2012), 407–424.
- [18] Li, J. and Cheng, Y. Linear barycentric rational collocation method for solving heat conduction equation, Numer. Methods Partial Differ. Equ. 37 (2021), 533–545.
- [19] Li, J. and Cheng, Y. Barycentric rational method for solving biharmonic equation by depression of order, Numer. Methods Partial Differ. Equ. 37 (2021), 1993–2007.
- [20] Li, M. and Huang, C. The linear barycentric rational quadrature method for auto-convolution Volterra integral equations, J. Sci. Comput. 78 (2019), 549–564.
- [21] Linz, P. Analytical and Numerical Methods for Volterra Equations, SIAM, Philadelphia, 1985.
- [22] Liu, H., Huang J. and He, X. Bivariate barycentric rational interpolation method for two dimensional fractional Volterra integral equations, J. Comput. Appl. Math. 389 (2021), 113339.
- [23] Luo, W.-H., Huang, T.-Z., Gu, X.-M. and Liu, Y. Barycentric rational collocation methods for a class of nonlinear parabolic partial differential equations, Appl. Math. Lett. 68 (2017), 13–19.

[24] Trefethen, L.N., et al. Chebfun Version 5.6.0, The Chebfun Development Team, http://www.chebfun.org (2016)

- [25] Trefethen, L.N. Is Gauss quadrature better than Clenshaw–Curtis? SIAM Rev. 50 (2008), 67–87.
- [26] Zhang, T. and Liang, H. Multistep collocation approximations to solutions of first-kind Volterra integral equations, Appl. Numer. Math. 130 (2018), 171–183.